

Assessment of diastolic chamber properties of the right ventricle by global fitting of pressure-volume data and conformational analysis of 3D + T echocardiographic sequences

C. Pérez del Villar¹, D. Rodríguez-Pérez², M. M. Desco², P. Martínez-Legazpi³, Y. Benito¹, A. Barrio¹, R. Yotti¹, J. Ortuño⁴, M. Ledesma⁴, F. Fernández-Avilés¹, J. Bermejo¹, J. C. Antoranz²

¹Hospital General Universitario Gregorio Marañón, Department of Cardiology, Madrid, Spain

²UNED, Física Matemática y de Fluidos, Madrid, Spain.

³University of California San Diego, Mechanical and Aerospace Engineering, La Jolla CA, United States

⁴Universidad Politécnica de Madrid, Biomedical Image Technology Group, Madrid, Spain

Keywords Diastole · Right ventricle · 3D echocardiography · Pressure-volume data

Purpose

Right ventricular (RV) dysfunction is a major prognosis determinant in many cardiovascular diseases. However, the physiological basis of RV diastolic function remains unclear [1]. Diastolic function is regulated by active and passive chamber properties. Active relaxation accounts for myofilament unbridging. Passive mechanical properties are derived from elastic chamber deformation when it is filled below or beyond its equilibrium volume (V_0 ; i.e. chamber volume at zero transmural pressure). Passive forces acting below V_0 account for elastic restoring forces, whereas those acting above V_0 are defined by ventricular stiffness. Currently, the analysis of pressure and volume (PV) data is indispensable for assessing diastolic chamber properties. Classical methods of PV data analysis focus on the characterization of relaxation and stiffness at specific times of diastole. Early diastole pressure-time exponential fitting characterizes relaxation whereas stiffness is estimated by fitting the curvilinear end-diastolic PV relationship from multiple beats during preload manipulation [2]. Recently, an algorithm based on global optimization has been validated to analyze left ventricular (LV) PV data providing most accurate indices of diastolic function by decoupling active and passive mechanical chamber properties [3]. The objectives of the present study were to characterize, for the first time in vivo, the relative contribution of RV active and passive diastolic chamber properties to RV filling and analyze their relationship with RV conformational changes during RV overload.

Methods

Thirteen minipigs were instrumented with a pressure-conductance catheter in RV. Acute preload reduction was induced with a balloon placed in the inferior vena cava (IVC). PV data were acquired during transient IVC occlusion during inotropic modulation, volume overload and during acute RV failure induced by infusion of *E. coli* lipopolysaccharide. 3D echocardiography was performed in each

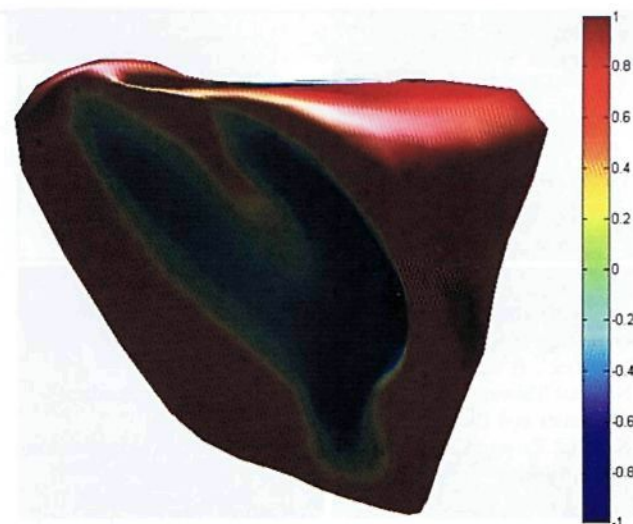


Fig. 1 Shape-index scale computing for a RV mesh at end diastole

phase. Indices of RV diastolic function were obtained with a numerical global optimization algorithm. Thus, diastolic pressure is defined as the resultant of adding active (P_a) and passive (P_p) forces acting throughout the full diastolic period. These pressure components are defined by relaxation constant (t), equilibrium volume (V_0), stiffness constants below and above V_0 (S_- and S_+) and volume asymptotes (V_m and V_d). 3D echocardiography RV images were analyzed off-line using commercial software and the inner surface meshes were further processed. After RV surface segmentation curvature parameters were calculated. Local minimum, maximum and mean curvatures, as well as shape-index (ratio of the maximum and minimum curvatures difference to the mean curvature) were computed for each triangle in the mesh (Fig. 1) [4]. Linear mixed-effects models (R, version 2.15.1) were used for data analysis, accounting for animal random effects.

Results

The interventions modulated RV hemodynamics as expected (see Table 1). The numerical algorithm converged in all data sets ($n = 224$). Passive restoring forces generated sub-atmospheric suction in all phases, significantly contributing to rapid filling. Remarkably, maintenance of suction despite severe acute RV overload was possible by shifting the passive PV relationship by increasing V_0 (see Table 1). This mechanism enhanced rapid filling by increasing the RA-RV pressure gradient and lowering RV diastolic pressures (Fig. 2) Conformational analysis demonstrated that both V_0 and the stiffness constant below V_0 (S_-) were significantly related to the degree of the RV septum bulging towards the LV at end-systole ($p < 0.05$). In turn, septal curvature was significantly related to the RV-LV transeptal pressure gradient ($p < 0.01$).

Conclusion

Diastolic pressure caused by passive elastic restoring forces is a major determinant of RV filling. During acute overload, the curvature of the interventricular septum determines the magnitude of these restoring

Table 1 Effects of acute hemodynamic interventions on RV function and diastolic properties

	Baseline	Exsanguination	Dehydration	Volume	Endotoxin (10 min)	Endotoxin (180 min)
Heart Rate (bpm)	92 (85 to 100)	84 (77 to 92)*	118 (110 to 126)*	99 (91 to 107)	88 (81 to 97)	114 (106 to 122)*
Cardiac Output (L/min)	2.3 (2.0 to 2.6)	2.1 (1.7 to 2.3)*	2.7 (2.4 to 3)*	2.9 (2.6 to 3.3)*	2.2 (1.9 to 2.5)	2.4 (2.0 to 2.7)
Peak RVP (mm Hg)	29.8 (25.1 to 34.5)	28.4 (23.7 to 33.1)	36.4 (31.4 to 41.3)*	42.4 (37.3 to 47.6)*	41.9 (37.1 to 46.7)*	45.5 (40.7 to 50.3)*
EDP (mm Hg)	5.4 (4.4 to 6.5)	6.9 (5.8 to 7.9)*	4.1 (3.0 to 5.2)	14.9 (13.7 to 16.1)*	9.8 (8.0 to 11.6)*	6.9 (5.8 to 7.9)*
EDV (ml)	47 (40 to 54)	48 (41 to 55)	42 (35 to 49)*	56 (49 to 63)*	53 (46 to 60)*	61 (54 to 68)*
RVEF (%)	0.53 (0.49 to 0.58)	0.49 (0.45 to 0.54)	0.57 (0.52 to 0.62)	0.55 (0.51 to 0.6)	0.46 (0.42 to 0.51)*	0.56 (0.51 to 0.61)*
t (ms)	41 (36 to 46)	39 (34 to 44)	29 (24 to 35)*	64 (59 to 70)*	40 (35 to 45)	46 (41 to 51)
V ₀ (ml)	30 (24 to 37)	29 (23 to 35)	28 (21 to 34)	32 (25 to 38)	31 (25 to 38)	45 (39 to 52)*
APV at V ₀ (mm Hg/ml)	0.3 (0.2 to 0.3)	0.3 (0.3 to 0.4)	0.2 (0.2 to 0.3)	0.5 (0.5 to 0.6)*	0.3 (0.2 to 0.3)	0.3 (0.2 to 0.3)

Values show the minimum, last effect (95% CI). Data showed median (interquartile range) for repeated measures within animal. * $p < 0.05$ vs. baseline. RVP, right ventricular pressure; RVEF, RV end-diastolic pressure; EDV, RV end-diastolic volume; RVEF, right ventricular ejection fraction; t, relaxation constant; V₀, equilibrium volume.

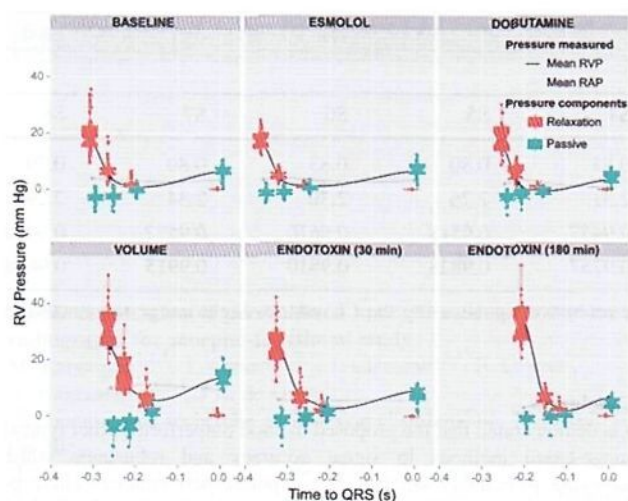


Fig. 2 Bar charts of active (in red) and passive (in blue) component of estimated pressure and mean measured pressure (black line) during diastole

forces. For the first time, these aspects of diastolic function can be analyzed in vivo by global optimization PV data analysis and shape conformational analysis of 3D + t echocardiographic sequences.

Acknowledgments

Authors are in debt with all the personnel of the Unit of Experimental Medicine and Surgery of the Hospital General Universitario Gregorio Marañón for their help in animal experiments. This study was supported by grants PI12/02885 and CM12/00273 (to CPV) from the Instituto de Salud Carlos III, Spain. CPV was partially supported by grants from the Fundación para Investigación Biomédica Gregorio Marañón, Spain.

References

- [1] Haddad F, Doyle R, Murphy DJ, Hunt SA. (2008) Right ventricular function in cardiovascular disease, part ii: Pathophysiology, clinical importance, and management of right ventricular failure. *Circulation*. 117:1717–1731
- [2] Burkhoff D, Mirsky I, Suga H. (2005) Assessment of systolic and diastolic ventricular properties via pressure–volume analysis: A guide for clinical, translational, and basic researchers. *Am J Physiol Heart Circ Physiol*. 289:H501–512
- [3] Bermejo J, Yotti R, Perez del Villar C, del Alamo JC, Rodriguez-Perez D, Martinez-Legazpi P, Benito Y, Antoranz JC, Desco MM, Gonzalez-Mansilla A, Barrio A, Elizaga J, Fernandez-Aviles F. (2013) Diastolic chamber properties of the left ventricle assessed by global fitting of pressure–volume data: Improving the gold standard of diastolic function. *J Appl Physiol*. 115:556–568
- [4] Koenderink JJ, Van Doorn AJ. (1992) Surface shape and curvature scales. *Image and Vision Computing*. 10:557–564